
Critical Parameters for Scalable Distributed Learning with Large Batches and Asynchronous Updates

Sebastian U. Stich
EPFL

Amirkeivan Mohtashami
EPFL

Martin Jaggi
EPFL

Abstract

It has been experimentally observed that the efficiency of distributed training with stochastic gradient (SGD) depends decisively on the batch size and—in asynchronous implementations—on the gradient staleness. Especially, it has been observed that the speedup saturates beyond a certain batch size and/or when the delays grow too large.

We identify a data-dependent parameter that explains the speedup saturation in both these settings. Our comprehensive theoretical analysis, for strongly convex, convex and non-convex settings, unifies and generalizes prior work directions that often focused on only one of these two aspects. In particular, our approach allows us to derive improved speedup results under frequently considered sparsity assumptions. Our insights give rise to theoretically based guidelines on how the learning rates can be adjusted in practice. We show that our results are tight and illustrate key findings in numerical experiments.

1 Introduction

Parallel and distributed machine learning training techniques have gained significant traction in recent years. A large body of recent work examined the benefits of parallel training in data centers (Dean et al., 2012; Goyal et al., 2017) or when scaling the training to millions of edge devices in the emerging federated learning paradigm (McMahan et al., 2017; Kairouz et al., 2019). However, many of these works reported diminishing efficiency gains when surpassing a certain critical level of parallelism. For instance, in mini-batch

SGD (Robbins and Monro, 1951; Zinkevich et al., 2010; Dekel et al., 2012), where the training is parallelized by evaluating a randomly sampled mini-batch of size b each iteration, near-linear optimal scaling is only possible for moderate batch sizes in practice. Recent studies report data-set dependent critical batch sizes beyond which the speedup saturates (Dean et al., 2012; Goyal et al., 2017; Shallue et al., 2019; Lee et al., 2020).

This saturation is not surprising when considering the extreme case of very large batches (larger than the training data set size), in which case SGD reduces to deterministic gradient descent (GD). It is known that training with GD cannot be accelerated by evaluating more than one gradient in parallel (Arjevani et al., 2020). This shows that the critical level of parallelism depends on the *stochasticity* of the task. Recent works introduced notions to measure stochastic gradient diversity on empirical risk minimization problems (Yin et al., 2018; Sankararaman et al., 2019). In this work, we consider more general stochastic problems, refine their notions and provide new insights.

Dekel et al. (2012) provide a concise analysis of mini-batch SGD, and argue that—theoretically—for optimal parallel speedup, the batch size should be chosen $\Theta(\frac{\sigma^2}{\epsilon})$, where σ^2 is a uniform (global) upper bound on the stochastic noise, and $\epsilon > 0$ the target accuracy. As a consequence, any *constant* batch size allows for near linear speedup¹ when the target accuracy is small enough. Analogous phenomena have been observed for asynchronous parallel methods (cf. Chaturapruek et al., 2015; Hannah and Yin, 2018). However, these observations can often not be corroborated in practice, where speedup saturates beyond certain batch size thresholds (Shallue et al., 2019). Reasons for this discrepancy could be, that in the context

¹We define near linear speedup as $T(b, \epsilon) \leq 2T(1, \epsilon)$, $\forall \epsilon > 0$, where $T(b, \epsilon)$ denotes the oracle complexity (number of stochastic gradient evaluations) of an algorithm with parallelism b (for instance mini-batch SGD with batch size b) to reach a certain accuracy ϵ on the considered problem instance. The constant in the definition could be replaced by an arbitrary other constant larger than one.

of machine learning applications we need to consider moderate values of the training-accuracy ϵ only (approximately n^{-1} , where n denotes the training data set size), and we cannot consider ϵ to be an arbitrarily small value (Bottou, 2010). Moreover, the uniform upper bound on the noise might be a too conservative parameter, as for instance in the context of over-parametrized problems the variance can vanish, i.e. $\sigma^2 \approx 0$ close to the optimum (Ma et al., 2018).

Based on founded theoretical arguments, we show that the optimal batch size scales as $\mathcal{O}(\frac{\sigma_*^2}{\epsilon} + M)$, where σ_*^2 is a bound on the variance close to stationary points only (and can be much smaller than the previously mentioned σ^2), and M a parameter we define later. This explains the optimal batch size in the important low-accuracy regime and matches with practical findings in terms of speedup saturation (cf. Figure 1) but also regarding optimal learning rate scaling (cf. Figure 2).

Interestingly, our findings are not limited to parallelism induced by large batches alone, but they also apply to settings where parallelism is caused by staleness (delayed gradient updates) or asynchrony.

Contributions. We study a broad variety of parallel versions of SGD, including mini-batch SGD, delayed SGD (Arjevani et al., 2020) and asynchronous HOGWILD! (Niu et al., 2011) in a unified way, and derive convergence rates for strongly-convex, convex, and the important non-convex setting. We identify a parameter that allows a tight interpretation of critical scaling parameters. In particular, we find that $\tau_{\text{crit}} := \mathcal{O}(\frac{\sigma_*^2}{\epsilon} + M)$, where σ_*^2 and M are data- and model-dependent constants, is a critical parameter that governs parallelism:

- We show that mini-batch SGD enjoys near-linear speedup up to a critical batch size $b_{\text{crit}} = \tau_{\text{crit}}$. As a practical guideline, our findings supports the widely-used *linear scaling rule* for the learning rate, but only up to the critical batch size b_{crit} .
- For asynchronous and delayed SGD we show strong linear speedup if the delays are not larger as τ_{crit} .
- As a particular novel insight, we prove that for problems with relative sparse gradient (measured by parameter $\Delta \leq 1$), a strong linear speedup can be attained as long as the delay (or batch size) $\tau = \mathcal{O}(\Delta^{-1})$. This improves prior best results by a factor of $\Delta^{-1/2}$ and is tight in general.
- We verify our findings in experiments and show that our identified parameters can explain speedup saturation observed in practice. We show this in a synthetic setup where we have tight control over the problem parameters, and further, we estimate the critical parameters on standard deep learning task.

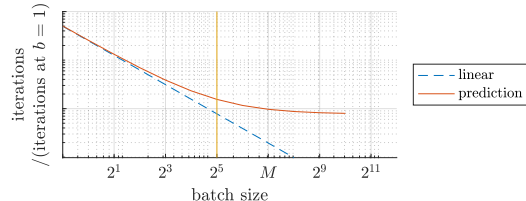


Figure 1: Predicted parallel speedup $\mathcal{O}(\frac{b+M}{b+bM})$, see Section 5. Relative number of iterations with batch size b vs. iterations with batch size $b = 1$, to reach the same target accuracy. The curve qualitatively matches with the empirical results of (Shallue et al., 2019).

2 Related Work

The seminal work of Bertsekas and Tsitsiklis (1989) provides strong foundations for parallel and distributed optimization with stochastic algorithms and discusses asynchronous algorithms for optimization with several parallel workers—without providing non-asymptotic convergence rates.

The parallel efficiency of asynchronous SGD methods was studied in (Tsitsiklis et al., 1986), using a parameter similar to our M considered here. Following the works of Langford et al. (2009); Niu et al. (2011); Dean et al. (2012), interest in the community renewed (Duchi et al., 2013; Mania et al., 2017; Leblond et al., 2018; Nguyen et al., 2019; Arjevani et al., 2020; Stich and Karimireddy, 2020), with particular focus on problems with sparse gradients (motivated by problems such as SVM, matrix completion, GLMs). Agarwal and Duchi (2011) showed that under restrictive ordering assumptions delayed SGD updates can have negligible asymptotic effect. This observation was corroborated under much weaker assumptions in (De Sa et al., 2015; Chaturapruek et al., 2015; Sra et al., 2016; Nguyen et al., 2019).

Dekel et al. (2012) provide a concise analysis of mini-batch SGD and argue theoretically about the optimal batch size and Friedlander and Schmidt (2012) propose exponentially increasing batch sizes on strongly-convex problems. Whilst these strategies yield near linear speedup, these schedules often do not align with practical needs, as discussed earlier. For constant batch sizes, it has been observed that linear speedup saturates beyond a certain threshold (Shallue et al., 2019), and several works aimed to express this saturation regime by data-dependent parameters, for instance by gradient diversity in (Yin et al., 2018; Chen et al., 2018) or as a function of the norm of the Hessian of the data in (Jain et al., 2018) for least square regression. Whilst these results are very close to ours, and convey a similar message—that larger diversity in stochastic gradients allows for increased levels of

parallelism—we extend their observations to more general settings.

The critical batch size is strongly linked the choice of the best learning rate. Our theorems suggest a learning rate scaling $\mathcal{O}(\frac{b}{b+M})$ which corroborates the popular linear scaling from (Goyal et al., 2017) but *only for* $b \leq M$, and the learning rate should be kept constant when b surpasses M .

3 Setup

We now describe the theoretical framework.

3.1 Optimization Problem

We consider the (stochastic) optimization problem

$$f^* := \min_{\mathbf{x} \in \mathbb{R}^d} f(\mathbf{x}), \quad (1)$$

where $f: \mathbb{R}^d \rightarrow \mathbb{R}$ is assumed to be L -smooth.

Assumption 1 (L -smoothness). *A differentiable function $f: \mathbb{R}^n \rightarrow \mathbb{R}$ with gradients satisfying:*

$$\|\nabla f(\mathbf{x}) - \nabla f(\mathbf{y})\| \leq L\|\mathbf{x} - \mathbf{y}\|, \quad \forall \mathbf{x}, \mathbf{y} \in \mathbb{R}^d. \quad (2)$$

Sometimes we will assume in addition that the objective function is convex.

Assumption 2 (μ -convexity). *A function $f: \mathbb{R}^n \rightarrow \mathbb{R}$ is μ -convex if for all $\mathbf{x}, \mathbf{y} \in \mathbb{R}^d$:*

$$f(\mathbf{y}) \geq f(\mathbf{x}) + \langle \nabla f(\mathbf{x}), \mathbf{y} - \mathbf{x} \rangle + \frac{\mu}{2}\|\mathbf{y} - \mathbf{x}\|^2. \quad (3)$$

When $\mu > 0$ this is commonly known as μ -strong-convexity. Our results can be extended to the weaker notion of Polyak-Łojasiewicz condition.

3.2 Stochastic Noise

We assume that for every point in $\mathbf{x} \in \mathbb{R}^d$ we can query a stochastic gradient $\mathbf{g}(\mathbf{x})$ of $f(\mathbf{x})$, that is

$$\mathbf{g}(\mathbf{x}) := \nabla f(\mathbf{x}) + \boldsymbol{\xi}(\mathbf{x}), \quad (4)$$

where $\boldsymbol{\xi}(\mathbf{x}) \in \mathbb{R}^d$ denotes the realization of a zero-mean random variable. We do in general not assume that the noise is independent of \mathbf{x} . For $\epsilon \geq 0$, we define

$$\sigma_\star^2 := \sup_{\|\nabla f(\mathbf{x})\|^2 \leq \epsilon} \mathbb{E}\|\boldsymbol{\xi}(\mathbf{x})\|^2.$$

For $\epsilon = 0$, this measures the noise at stationary points, and for $\epsilon = \infty$ this recovers the standard notion assuming uniformly (globally) bounded noise on \mathbb{R}^d . We further define

$$M := \sup_{\|\nabla f(\mathbf{x})\|^2 > \epsilon} \frac{\mathbb{E}\|\boldsymbol{\xi}(\mathbf{x})\|^2}{\|\nabla f(\mathbf{x})\|^2}.$$

We will drop the subscript in σ^2 whenever there is no ambiguity. These two definitions imply:

Property 3 (noise). *There exist parameters $M \geq 0, \sigma^2 \geq 0$ such that for every gradient oracle as in (4) and for all $\mathbf{x} \in \mathbb{R}^d$:*

$$\mathbb{E}[\boldsymbol{\xi}(\mathbf{x})] = \mathbf{0}_d, \quad \mathbb{E}\|\boldsymbol{\xi}(\mathbf{x})\|^2 \leq M\|\nabla f(\mathbf{x})\|^2 + \sigma^2. \quad (5)$$

In related works, similar inequalities as (5) are sometimes stated as an assumption (Tsitsiklis et al., 1986; Bottou et al., 2018), e.g. for $M = 0$ we recover the uniformly bounded noise assumption. Furthermore, it has been proved that this property always holds under certain assumptions (Cevher and Vü, 2019).

3.3 Algorithm

We now introduce an algorithmic template that can capture a broad class standard SGD implementations, such as mini-batch SGD, or asynchronous SGD. For simplicity, we assume a constant stepsize γ throughout the iterations. This formulation is identical to the description of the HOGWILD! algorithm as for instance stated in (Mania et al., 2017; Leblond et al., 2018).²

Algorithm 1 PARALLEL SGD TEMPLATE

```

1: Initialization: shared variable  $\mathbf{x} = \mathbf{x}_0 \in \mathbb{R}^d$ 
2: for  $t = 0, \dots, T$  keep doing in parallel
3:    $\mathbf{x}_t \leftarrow$  inconsistent read of  $\mathbf{x}$ 
4:   sample stochastic gradient  $\mathbf{g}_t := \mathbf{g}(\mathbf{x}_t)$ 
5:   for  $v \in \text{supp}(\mathbf{g}_t) \subseteq [d]$  do
6:      $[\mathbf{x}]_v \leftarrow [\mathbf{x}]_v - \gamma[\mathbf{g}_t]_v$   $\triangleright$  atomic coordinate write
7: end parallel loop
    
```

Special cases. First, we remark that the standard mini-batch SGD algorithm with batch size $b \geq 1$ can be cast into the form of Algorithm 1: Consider b parallel processes, which all (consistently) read the state variable \mathbf{x}_t , compute independent stochastic gradients \mathbf{g}_{t+i} , for $i \in \{0, \dots, b-1\}$, and then apply the updates in a synchronous fashion, such that it holds $\mathbf{x}_{t+b} = \mathbf{x}_t - \gamma \sum_{i=0}^{b-1} \mathbf{g}_{t+i}$.

In addition, our framework also covers a broad range of asynchronous SGD implementations. The parameter \mathbf{x} is allowed to inconsistently change during the read in line 3 as other processes could be writing to \mathbf{x} concurrently (line 6). As the processes also do not necessarily need to read (or write) the coordinates of \mathbf{x} in order (allowing for low-level system optimization) we have to be careful in the analysis with the definition of \mathbf{x}_t .

Global Ordering: “After read” approach. We follow (Leblond et al., 2018) to define a global order-

²In the earlier version studied in (Niu et al., 2011) only one single coordinate is updated per iteration (and the others discarded).

ing of the iterates of Algorithm 1 and update the (virtual) counter t after each complete read of the shared variable \mathbf{x} . A key property to be noted is that it holds

$$\mathbb{E}[\mathbf{g}(\mathbf{x}_t) \mid \mathbf{x}_t] = \nabla f(\mathbf{x}_t),$$

as the stochastic gradient is sampled only after \mathbf{x}_t is read completely. This might be obvious in our notation, though note that for instance in finite sum settings one might be tempted—for efficiency reasons—to sample an index $i \sim_{\text{u.a.r.}} [n]$ before reading \mathbf{x} and then only read the coordinates that are relevant to compute $\nabla f_i(\mathbf{x})$. However, when using this shortcut, \mathbf{x}_t in general depends on the randomness used to generate the stochastic gradient and $\mathbb{E}[\mathbf{g}(\mathbf{x}_t)] \neq \nabla f(\mathbf{x}_t)$ in general. See also (Leblond et al., 2018) for a thorough discussion of this issue.

A key assumption for our analysis is—as in prior work—that the writes on \mathbf{x} cannot overwrite \mathbf{x} arbitrarily, but only add or subtract values.

Assumption 4 (Atomic update). *The update of the coordinate $[\mathbf{x}]_v$ on line 6 is atomic.*

In view of Assumption 4 it follows that each iterate \mathbf{x}_t can be expressed as

$$\mathbf{x}_t = \mathbf{x}_0 - \gamma \sum_{k=0}^{t-1} \mathbf{J}_k^t \mathbf{g}_k \quad (6)$$

for diagonal matrices $\mathbf{J}_k^t \in \mathbb{R}^{d \times d}$, $k < t$, with

$$(\mathbf{J}_k^t)_{vv} = \begin{cases} 1 & \text{if } [\mathbf{g}_k]_v \text{ written before } [\mathbf{x}_t]_v \text{ was read,} \\ 0 & \text{otherwise.} \end{cases}$$

Note that due to the concurrent nature of the writes of the processes to the shared vector, and by the fact that reads on line 3 are not necessarily reading the coordinates in the same order, we can in general not assume $(\mathbf{J}_k^t)_{vv} \geq (\mathbf{J}_k^{t+1})_{vv}$. However, it is standard to assume bounded overlaps, i.e. a maximal delay during which iterations can overlap. This parameter captures the level of parallelism.

Definition 1 (degree of parallelism). *Define (with the convention that the maximum over the empty set is zero):*

$$\tau := \sup_{t \geq 0} \max_{k < t, \mathbf{J}_k^t \neq \mathbf{I}_d} |t - k| + 1.$$

The parameter τ unifies common notions of parallelism: for instance in mini-batch SGD the parameter τ is identical to the batch size b . For asynchronous methods with delays and staleness, the parameter τ is a uniform bound on the largest delay, recovering notions as in (Niu et al., 2011; Leblond et al., 2018). While we do not investigate the mini-batch asynchronous setting explicitly, our theory also applies to the mini-batch asynchronous setting. In this case, the critical parameter would be, $b \cdot \tau$, i.e. the multiplication of the batch size and the delay.

4 Main Results

We now state our main convergence result.

Theorem 1. *Let Assumptions 1 and 4 hold, let (M, σ^2) denote parameters with Property 3, and define the critical stepsize $\gamma_{\text{crit}} := \frac{1}{10L(M+\tau)}$. For any $\epsilon > 0$, there exists a stepsize $\gamma \leq \gamma_{\text{crit}}$ such that Algorithm 1 reaches an ϵ -approximate solution after at most the following number of iterations T :*

Non-Convex: $\min_{t \in [T]} \|\nabla f(\mathbf{x}_t)\|^2 \leq \epsilon$ after

$$\mathcal{O}\left(\frac{\sigma^2}{\epsilon^2} + \frac{M + \tau}{\epsilon}\right) \cdot LF_0$$

iterations with $\gamma = \mathcal{O}(\min\{\gamma_{\text{crit}}, (\frac{F_0}{\sigma^2 T})^{1/2}\})$, where $F_0 := f(\mathbf{x}_0) - f^*$.

Strongly convex: *If additionally Assumption 2 holds with $\mu > 0$, then $\mathbb{E}[f(\bar{\mathbf{x}}_T) - f^* + \mu \|\mathbf{x}_T - \mathbf{x}^*\|^2] \leq \epsilon$ after*

$$\tilde{\mathcal{O}}\left(\frac{\sigma^2}{\mu \epsilon} + \frac{L(M + \tau)}{\mu}\right)$$

iterations with $\gamma = \tilde{\mathcal{O}}(\min\{\gamma_{\text{crit}}, \frac{1}{\mu T}\})$, ($\tilde{\mathcal{O}}(\cdot)$ suppressing log factors) and

Convex: when $\mu = 0$:

$$\mathcal{O}\left(\frac{\sigma^2}{\epsilon^2} + \frac{L(M + \tau)}{\epsilon}\right) \cdot R_0^2,$$

with $\gamma = \mathcal{O}(\min\{\gamma_{\text{crit}}, (\frac{R_0^2}{\sigma^2 T})^{1/2}\})$, where $R_0^2 = \|\mathbf{x}_0 - \mathbf{x}^*\|^2$. Here $\bar{\mathbf{x}}_T$ denotes a weighted average of the iterates \mathbf{x}_t , $t \in \{0, \dots, T\}$ and \mathbf{x}_T the last iterate.

The proof of this theorem follows from (Stich and Karimireddy, 2020) with only minor modifications of their proof. This earlier work did only consider the case when the degree of parallelism is exactly τ throughout the optimization and did not consider coordinate-wise overwrites.

For many special cases, Theorem 1 recovers known convergence bounds. For instance for $M = \sigma^2 = 0$, the case of (deterministic) *gradient descent*, it is well known that for a stepsize $\gamma = \frac{1}{L}$ the above convergence bounds can be reached, and in general not improved without acceleration techniques (Nesterov, 2004). Similarly, for synchronous SGD with uniformly (globally) bounded noise ($M = 0, \tau = 1$), the dependency on σ^2 can in general not be improved and matches known results (Nemirovski and Yudin, 1983).

By considering the deterministic gradient descent setting, it is also clear that the critical stepsize cannot be significantly (up to constant factors) larger than $\frac{1}{L\tau}$, as for any batch size $b = \tau$, $\frac{1}{b} \sum_{i=0}^{\tau-1} \nabla f(\mathbf{x}) \equiv \nabla f(\mathbf{x})$, and the stepsize in Algorithm 1 has to be scaled by $\frac{1}{b}$.

5 Large Batch Training

We will discuss these results in the following two sections. Whilst we focus in particular on large batch training in this section, and on asynchronous methods under sparsity assumption in the next section, our discussions are interchangeable, as we measure parallelism by a universal parameter $b = \tau$ and our results are not tied to a particular scheme.

Speedup and critical batch size. In Theorem 1 we depict the oracle complexity $T(b, \epsilon)$, that is the number of gradient evaluations needed to reach a target accuracy ϵ . In parallel implementations, for instance in mini-batch SGD with batch size b , we can gain (up to)³ a factor of b by computing b gradients in parallel. Therefore, the parallel running time is $\frac{1}{b}T(b, \epsilon)$, and the *parallel speedup* over a single thread implementation $T(1, \epsilon)$ is

$$\frac{T(1, \epsilon)}{\frac{1}{b}T(b, \epsilon)} = b \cdot \mathcal{O}\left(\frac{\sigma_*^2/\epsilon + M + 1}{\sigma_*^2/\epsilon + M + b}\right),$$

for all settings considered in Theorem 1 (ignoring L). Here the first factor, b , indicates the potential linear speedup gained by the level of parallelism, and the second factor the slowdown from the increased number of required steps (gradient computations). We have *near-linear* speedup when the second factor is bounded by a constant, for instance for any batch size not exceeding $b \leq \mathcal{O}(1) \cdot b_{\text{crit}}$, relative to the *critical batch size* defined as

$$b_{\text{crit}} := \frac{\sigma_*^2}{\epsilon} + M + 1.$$

As we are in particular interested in the low-accuracy regime, i.e. the case when σ_*^2 is small or ϵ large (cf. Bottou, 2010; Ma et al., 2018), the constant term M is dominating in these bounds. In Figure 2 (left) we illustrate this speedup value depending on b .

For the special case of deterministic problems, where $M = \sigma_*^2 = 0$, the critical batch size is $b_{\text{crit}} = 1$ (as expected). Any level of parallelism increases the number of gradient computations linearly, as all parallel threads compute identical gradients. On the other hand, for any stochastic problem with $\sigma_*^2 > 0$, we see that the critical batch size can be unbounded. That is, stochastic problems can in principle be parallelized arbitrarily well in the asymptotic regime (see also Chaturapruek et al., 2015; Hannah and Yin, 2018; Nguyen et al., 2019). However, as mentioned before, this regime might not be reached in practice.

³We ignore communication overheads in our discussion.

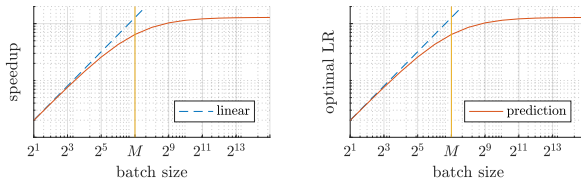


Figure 2: Predicted parallel speedup $\mathcal{O}(b \cdot \frac{M+1}{M+b})$ in the low-accuracy regime (left). Optimal learning rate (right).

Learning rate. The convergence results in Theorem 1 depend crucially on the choice of the stepsize, i.e. the near-linear speedup can only be reached when the learning rate is optimally tuned. In particular, for the low-accuracy regime, the learning rate should be chosen as large as possible for the fastest convergence, but smaller than the critical value, $\gamma_{\text{crit}} = \mathcal{O}(\frac{1}{L(M+b)})$ that ensures convergence. Note that the critical stepsize is nearly constant for batch sizes $1 \leq b \leq M$ below the critical batch size.

In many implementations of mini-batch SGD, the batch gradients are *averaged* (opposed to just summation in Algorithm 1):

$$\mathbf{x}_{t+b} := \mathbf{x}_t - \frac{\gamma_{\text{mb}}}{b} \sum_{i=0}^{b-1} \mathbf{g}_{t+i},$$

thereby reducing the effective stepsize $\gamma = \frac{\gamma_{\text{mb}}}{b}$ by a factor of b . However, in the linear speedup regime the effective steps size should not decrease b fold, hence γ_{mb} must be scaled by b (*linear scaling rule*). This explains the linear scaling rule widely used in deep learning (but not learning rate warmup). Our theory also explains why the linear scaling does not apply beyond the critical regime $b \gg b_{\text{crit}}$. We illustrate this scaling in Figure 2 (right).

Comparison to Gradient Diversity. Yin et al. (2018) introduced the notion of gradient diversity for finite-sum structured problems to determine the critical batch size. As their parameter depends on the number of components (data points in the training data set) it cannot be extended to the stochastic setting considered here. However, they also consider a scaled version, the *batch size bound*

$$B_S(\mathbf{x}) := \frac{\mathbb{E}\|\mathbf{g}(\mathbf{x})\|^2}{\|\nabla f(\mathbf{x})\|^2} = 1 + \frac{\mathbb{E}\|\boldsymbol{\xi}(\mathbf{x})\|^2}{\|\nabla f(\mathbf{x})\|^2}$$

which does not implicitly depend on the dataset size. Under our assumptions in Property 3, and further assuming $\|\nabla f(\mathbf{x})\|^2 \geq \epsilon$, we see that $B_S(\mathbf{x}) \leq b_{\text{crit}}$, however, for points \mathbf{x} with $\|\nabla f(\mathbf{x})\|^2 \leq \epsilon$ the value B_S can be arbitrarily larger than b_{crit} . Besides this difference, we observe that our critical batch size extends the notion of the batch size bound defined through gradient diversity only on empirical risk minimization problems to the more general class of stochastic problems.

6 Relative Sparsity

A line of work studied the speedup efficiency of SGD in terms of the (relative) sparsity of the stochastic gradients (we compare to these works in Table 1). Whilst in deep learning settings the stochastic gradients are in general not sparse, such assumptions are well motivated for instance in applications with generalized linear models, where gradients follow the same sparsity patterns as the data.

6.1 Speedup with sparsity

For a vector $\mathbf{x} \in \mathbb{R}^d$ let $\text{supp}(\mathbf{x}) \in 2^{[d]}$ denote the support of \mathbf{x} , i.e. the set of coordinates where \mathbf{x} is non-zero. We now define a quantity that measures the sparsity of the stochastic gradients. Our definition generalizes the notion used in (Leblond et al., 2018) that was only defined for finite-sum structured objectives.

Definition 2 (Δ -sparsity). *Let $\mathbb{1}_X$ denote the indicator function of the event X . Define $\Delta \leq 1$ as*

$$\Delta := \sup_{\mathbf{x} \in \mathbb{R}^d} \max_{v \in [d]} \mathbb{E}_{\mathbf{g}(\mathbf{x})} [\mathbb{1}_{v \in \text{supp}(\mathbf{g}(\mathbf{x}))}]. \quad (7)$$

In other words, Δ is a uniform upper bound on the probability that a given coordinate $v \in [d]$ is non-zero for a (random) stochastic gradient $\mathbf{g}(\mathbf{x})$ at any $\mathbf{x} \in \mathbb{R}^d$.

Examples. A notable example are (random) coordinate descent methods, where we have $\Delta = \frac{1}{n}$, as every stochastic gradient is sparse. However, note that our definition does not measure sparsity alone. For instance, for a problem defined as $f(\mathbf{x}) := \frac{1}{2} \|\mathbf{x}\|_1^2$ in ambient dimension d , with stochastic gradients $\mathbf{g}(\mathbf{x}) = (\|\mathbf{x}\|_1 + u) \cdot \mathbf{e}_1$, where $u \sim \mathcal{N}(0, \sigma^2)$ is a Gaussian random variable, we have $\Delta = 1$, as the first coordinate is almost surely non-zero in every stochastic gradient. For the special case of finite sum structured problems, $f(\mathbf{x}) = \frac{1}{n} \sum_{i=1}^n f_i(\mathbf{x})$ our definition recovers the notion in (Leblond et al., 2018). To see this, let $S_i := \cup_{\mathbf{x} \in \mathbb{R}^d} \text{supp}(\nabla f_i(\mathbf{x}))$ denote the support of ∇f_i . As in (Niu et al., 2011; Leblond et al., 2018) we introduce $\Delta_r := \max_{v \in [d]} |\{i : v \in S_i\}|$, the maximum number of data points with a specific feature (coordinate) and normalize $\Delta := \Delta_r/n$. We observe that Δ by definition is an upper bound on the probability that a particular coordinate $v \in [d]$ is contained in the support S_i of a ∇f_i chosen uniformly at random. Hence, in the special case of finite sum structured problems our Definition 2 coincides with the literature (Niu et al., 2011; Mania et al., 2017; Leblond et al., 2018).

Key observation. Whilst prior work utilized the sparsity assumption for refining and tightening inequalities that arise in the convergence proof of SGD,

we depart from this approach here. Instead, we show how improved convergence estimates directly follow from Theorem 1. For this, we observe that the sparsity correlates with the variance, i.e. high sparsity implies high variance.

Lemma 1. *Let $X \in \mathbb{R}$ be a real random variable, with $\Pr[X \neq 0] \leq \Delta$. Then $|\mathbb{E}X|^2 \leq \Delta \cdot \mathbb{E}|X|^2$.*

Proof. By direct calculation, we verify:

$$\begin{aligned} |\mathbb{E}X|^2 &= |\Pr[X=0] \cdot 0 + \Pr[X \neq 0] \cdot \mathbb{E}[X | X \neq 0]|^2 \\ &= \Pr[X \neq 0]^2 \cdot |\mathbb{E}[X | X \neq 0]|^2 \\ &\leq \Pr[X \neq 0]^2 \cdot \mathbb{E}[|X|^2 | X \neq 0] \\ &= \Pr[X \neq 0] \cdot \left(0 + \Pr[X \neq 0] \cdot \mathbb{E}[|X|^2 | X \neq 0]\right) \\ &= \Pr[X \neq 0] \cdot \mathbb{E}|X|^2 \leq \Delta \cdot \mathbb{E}|X|^2, \end{aligned}$$

with Jensen's inequality and the assumption. \square

Corollary 2. *Let $\mathbf{g}(\mathbf{x})$ be a stochastic gradient with $\mathbb{E}_{\mathbf{g}(\mathbf{x})} = \nabla f(\mathbf{x})$ and with $\Delta \leq 1$ relative sparsity. Then*

$$\mathbb{E}_{\mathbf{g}(\mathbf{x})} \|\mathbf{g}(\mathbf{x}) - \nabla f(\mathbf{x})\|^2 \geq \left(\frac{1-\Delta}{\Delta}\right) \|\nabla f(\mathbf{x})\|^2.$$

Proof. Applying Lemma 1 coordinate-wise, we obtain

$$\|\nabla f(\mathbf{x})\|^2 \leq \Delta \cdot \mathbb{E}_{\mathbf{g}(\mathbf{x})} \|\mathbf{g}(\mathbf{x})\|^2, \quad (8)$$

and the claim follows by the bias-variance decomposition,

$$\begin{aligned} \mathbb{E}_{\mathbf{g}(\mathbf{x})} \|\mathbf{g}(\mathbf{x}) - \nabla f(\mathbf{x})\|^2 &= \mathbb{E}_{\mathbf{g}(\mathbf{x})} \|\mathbf{g}(\mathbf{x})\|^2 - \|\nabla f(\mathbf{x})\|^2 \\ &\stackrel{(8)}{\geq} \left(\frac{1}{\Delta} - 1\right) \|\nabla f(\mathbf{x})\|^2. \quad \square \end{aligned}$$

Consequences. For problems where the gradient norm $\|\nabla f(\mathbf{x})\|^2$ is not uniformly bounded over \mathbb{R}^d , we conclude that it must hold $M \geq \frac{1-\Delta}{\Delta}$ in Property 3. Hence, we see that we get linear speedup as long as $\tau\Delta \leq 1 - \Delta$. As highlighted in Table 1, our rates improve over the best previously known condition for speedup, $\Delta = \mathcal{O}(\tau^{-1/2})$, from (Leblond et al., 2018).

Dependence on $\tau\Delta$ is best possible. We argue that the speedup condition $\Delta = \mathcal{O}(\tau^{-1})$ cannot further be improved. To show this, we construct a problem instance for which SGD cannot achieve linear speedup if $\Delta \geq \omega(\tau^{-1})$ (i.e., asymptotically, $\Delta\tau \gg 1$).

First, consider a L -smooth, μ -strongly convex function $F: \mathbb{R}^d \rightarrow \mathbb{R}$. It is well known, that gradient descent with batch size τ cannot benefit from the parallelism and needs $\Omega(\tau)$ iterations in general to reach a target accuracy ϵ (chosen sufficiently small). As argued earlier in Section 5, this linear slowdown is expected, and not improvable.

Table 1: Comparison of convergence bounds for asynchronous SGD with delay τ . Early works relied on a bounded gradient assumption which was removed in (Nguyen et al., 2019), showing sublinear $\mathcal{O}(\frac{1}{\sqrt{\epsilon}})$ convergence when $\sigma^2 = 0$, and Leblond et al. (2018) are the first to show near linear speedup.

Asynchronous SGD reference	Convergence Rate ($\ \mathbf{x}_t - \mathbf{x}^*\ ^2 \leq \epsilon$)
	<i>bounded gradient assumption</i> $\ \mathbf{g}_t\ ^2 \leq G^2$
Niu et al. (2011)	$\tilde{\mathcal{O}}\left(\frac{LG^2(1+\tau\rho+\tau^2\Omega\sqrt{\Delta})}{\mu^2\epsilon}\right)^a$
De Sa et al. (2015)	$\tilde{\mathcal{O}}\left(\frac{G^2}{\mu^2\epsilon} + \frac{LG\tau}{\mu^2\sqrt{\epsilon}}\right)$
Chaturapruek et al. (2015)	$\mathcal{O}\left(\frac{G^2}{\mu^2\epsilon} + C\right)^b$
Mania et al. (2017)	$\tilde{\mathcal{O}}\left(\frac{G^2(1+\tau\Delta)}{\mu^2\epsilon} + \tau + \tau^2\Delta\right)$
Nguyen et al. (2019)	$\tilde{\mathcal{O}}\left(\frac{\sigma^2}{\mu^2\epsilon} + \frac{\sqrt{(1+\sqrt{\Delta}\tau)(1+\tau)(\sigma+LR_0)L}}{\mu^2\sqrt{\epsilon}}\right)$
Leblond et al. (2018)	lin.-speedup for $\tau = \mathcal{O}(\min\{\frac{L}{\mu}, \frac{1}{\sqrt{\Delta}}\})$
this paper	lin.-speedup for $\tau = \mathcal{O}(\frac{1}{\Delta})$

^a $\rho \leq 1$ and Ω are additional parameters measuring sparsity of the gradients, see (Niu et al., 2011).

^b $C = C(L, \mu, \tau)$ is an unspecified constant (asymptotic analysis only).

Let us assume w.l.o.g. that Δ is such that $B := \Delta^{-1}$ is an integer, and for the dimension $D = Bd$ define the block-separable function $f: \mathbb{R}^D \rightarrow \mathbb{R}$ as $f(\mathbf{x}) = \sum_{i=1}^B F([\mathbf{x}]_{B_i})$, where $[\mathbf{x}]_{B_i}$ denotes the projection of $\mathbf{x} \in \mathbb{R}^D$ to the i -th block of d coordinates. A Δ -sparse, unbiased stochastic gradient of f can be defined by $\mathbf{g}(\mathbf{x}) = B \cdot \nabla F([\mathbf{x}]_{B_i}) \mathbf{e}_{B_i}$ where $i \sim_{\text{u.a.r.}} [B]$ denotes a uniformly at random chosen block, and $\mathbf{e}_{B_i} \in \mathbb{R}^D$ the indicator vector of this block.

Suppose now, that there exists a stepsize γ , such that SGD with batch size $\Delta\tau$ finds an ϵ -approximate solution \mathbf{x}_T in $o(\Delta\tau)$ iterations. This means, that for each separable problem instance the condition $F([\mathbf{x}_T]_{B_i}) - F^* \leq \epsilon$ could be reached with only $o(\tau)$ updates per block (in expectation). This is not possible in general, as argued above.

6.2 Diversity-inducing mechanisms

Following the observation that problems with high sparsity allow for increased parallelism, one might wonder whether it is possible to accelerate training by artificially inducing sparsity. Such techniques were discussed in (Yin et al., 2018; Candela et al., 2019). For instance, by artificially sparsifying stochastic gradients \mathbf{g}_t with a mask \mathbf{M}_α , $\mathbb{E}\mathbf{M}_\alpha = \mathbf{I}_d$, the stochastic gradients become sparse, with $\Delta = \alpha^{-1}$ for a tune-able parameter $\alpha \geq 1$ (Alistarh et al., 2017).

Consider a problem where the baseline—non-sparsified SGD—converges as $\mathcal{O}(\tau + 1)$, i.e. not allowing any parallelism beyond $\tau = \mathcal{O}(1)$. With unbiased sparsified gradients, SGD now enjoys the convergence bound $\mathcal{O}(\tau + \alpha)$, tolerating parallelism up to $\tau = \mathcal{O}(\alpha)$. However, when comparing this rate with the baseline re-

sult, we observe that even with parallelism τ , there is no speedup that can be realized, as the total number of iterations increased by α when sparsifying the gradients. This means that our theoretical analysis presented here cannot confirm the effectiveness of artificial sparsification as proposed in (Candela et al., 2019) in general, though there is of course a possibility left that in special cases positive effects of sparsification can be observed in practice, or with modified versions of SGD (Alistarh et al., 2018).

7 Experiments

In the previous sections we argued theoretically that parallelism up to the critical level $\tau = \mathcal{O}(\frac{\sigma^2}{\epsilon} + M)$ can yield linear speedup in parallel computation time. In this section, we experimentally verify this claim.

In the main paper we focus mainly on mini-batch SGD with varying batch sizes, and provide additional experiments in the appendix for asynchronous versions of SGD (including Hogwild!), with different delay patterns.

7.1 Scaling on controlled problem instance

First, we consider a family of controlled problem instances, corresponding to regularized linear regression problems, where we can control the noise (such as to control the parameter M). We consider the quadratic function $f: \mathbb{R}^d \rightarrow \mathbb{R}$,

$$f(\mathbf{x}) := \frac{1}{2} \langle A\mathbf{x}, \mathbf{x} \rangle + \frac{\lambda}{2} \|\mathbf{x}\|^2,$$

for $d = 20$, $\lambda = 0.2$, and band-diagonal matrix A with $[-\mathbf{1}_{d-1}, \mathbf{21}_d, -\mathbf{1}_{d-1}]$ on the diagonals. Without regularization (and without noise) this is a numerically challenging problem for first order methods (cf. Nesterov, 2004); with regularization the condition number reduces to approximately $\kappa \leq 19$. We define stochastic gradients with $\mathbf{u} \sim \mathcal{N}(\mathbf{0}, M\|\nabla f(\mathbf{x})\|^2 \cdot I_d)$ as

$$\mathbf{g}(\mathbf{x}) := \nabla f(\mathbf{x}) + \mathbf{u},$$

thus it holds $\mathbb{E}\|\mathbf{g}(\mathbf{x}) - \nabla f(\mathbf{x})\|^2 \leq M\|\nabla f(\mathbf{x})\|^2$.

In Figure 3 we depict the number of iterations required by mini-batch SGD to reach the target accuracy $\frac{1}{d}\|\mathbf{x}_t\| \leq 0.1$, for $\mathbf{x}_0 = 10 \cdot \mathbf{1}_d$, and for the best choice of stepsize (tuned over a logarithmic grid $\gamma \in \frac{1.1}{1+M} \cdot \{2^{-1}, \dots, 2^{-20}\}$, optimal values are always different from the largest or smallest value in this grid). We observe that the value M provides a lower bound on the level of parallelism that enjoys linear speedup, tracking the speedup saturation in the right order of magnitude, but slightly too conservative on this family of problem instances. Similar observations also hold

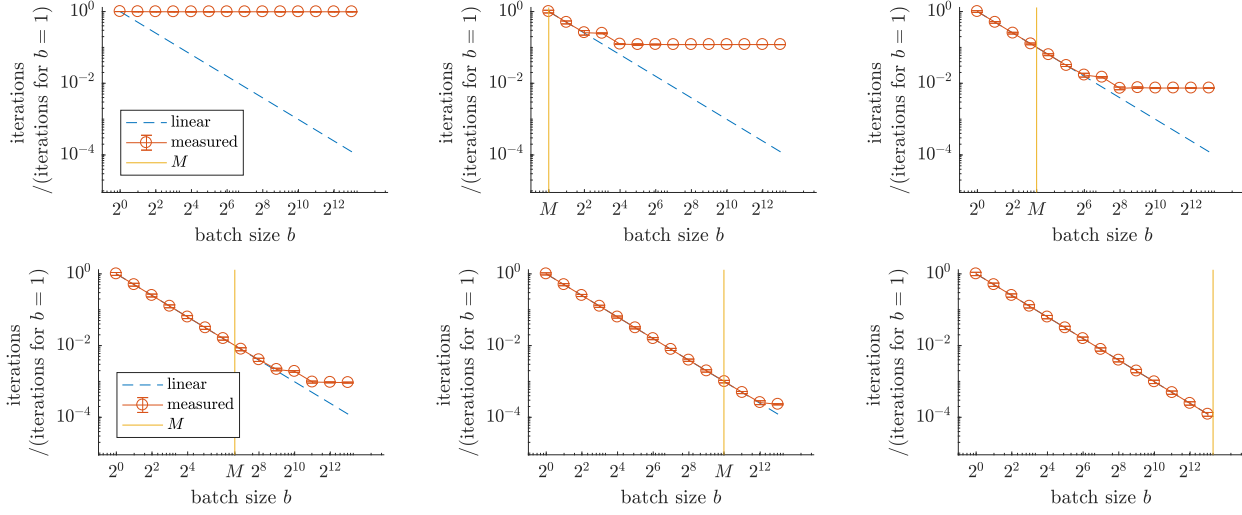


Figure 3: **Mini-batch SGD. Batch sizes smaller than M enjoy linear speedup.** Parallel speedup for various batch sizes $b \in \{2^0, \dots, 2^{14}\}$ and problem instances with $M \in \{0, 1, 10\}$ (top) and $M \in \{100, 1000, 10000\}$ (bottom), on the synthetic optimization problem described in Section 7.1. Plots depict number of iterations (i.e. parallel running time $\frac{1}{\epsilon}T(b, \epsilon)$), normalized by $T(1, \epsilon)$, required to reach the target accuracy with tuned optimal learning rates.

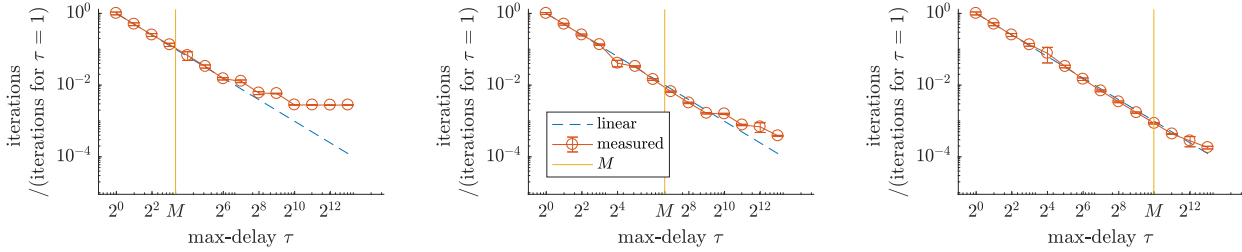


Figure 4: **Asynchronous SGD (Hogwild!).** Parallel speedup for delay parameters $\tau \in \{2^0, \dots, 2^{14}\}$ and problem instances with $M \in \{10, 100, 1000\}$ for the same problem setup as in Figure 3. See Appendix B.3 for further details.

for asynchronous methods, as displayed in Figure 4 (for more details we refer to Appendix B.3 and B.4).

7.2 Measuring the critical batch size on deep learning tasks

We now aim to understand whether our proposed critical batch sizes correlate with speedup saturation observed in practice (Shallue et al., 2019). We consider image classification for the CIFAR-10 (Krizhevsky and Hinton, 2009) dataset with ResNet-8 and ResNet-18 (He et al., 2016) architectures. We train these models for 200 epochs using mini-batch SGD with a momentum of 0.9, and $5 \cdot 10^{-4}$ weight decay.

As a heuristic measure of the critical batch size, we are tracking the evolution of the estimator

$$\hat{b}(\mathbf{x}) := 1 + \frac{\mathbb{E}\|\mathbf{g}(\mathbf{x}) - \nabla f(\mathbf{x})\|^2}{\|\nabla f(\mathbf{x})\|^2 + \hat{\epsilon}_T}, \quad (9)$$

where $\hat{\epsilon}_T$ is an estimate of the gradient $\|\nabla f(\mathbf{x}_T)\|^2$ at the end of training, measured by taking the average

over the last 10 epochs: $\hat{\epsilon}_T = \frac{1}{10} \sum_{i=0}^9 \|\nabla f(\mathbf{x}_{T-i \cdot n})\|^2$, where n is the training data set size, and T the final iteration index.⁴

In Figure 5 we show the evolution of $\hat{b}(\mathbf{x})$ when training on ResNet-18 for different batch sizes. Additionally, we investigate the effect of training with and without batch normalization with 256 batch size. We use 0.01 step size and do not apply any learning rate decay. The estimated value saturates around 5000, matching with typically observed saturation levels for all batch sizes except for $b = 16$, which is the only batch size not converging to a high accuracy.

We see that batch norm changes the optimization landscape and the training trajectory. Without batch norm, the estimated critical scaling parameter is much

⁴We show in Appendix B.1 that

$$\hat{b}(\mathbf{x}) \leq 1 + \frac{\sigma_*^2}{\max\{\|\nabla f(\mathbf{x})\|^2, \hat{\epsilon}_T\}} + M \leq 4 \sup_{\mathbf{x} \in \mathbb{R}^d} \hat{b}(\mathbf{x}),$$

and hence $\hat{b}(\mathbf{x})$ can be seen as a local estimate of b_{crit} for $\epsilon = \max\{\|\nabla f(\mathbf{x})\|^2, \hat{\epsilon}_T\}$.

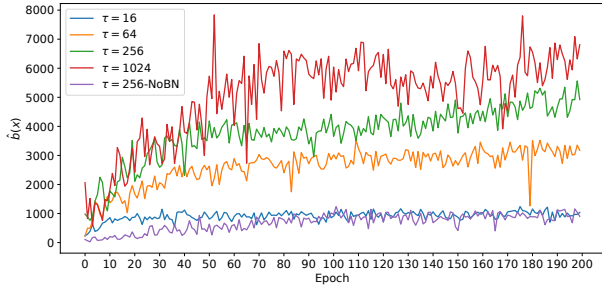


Figure 5: Evolution of the critical parameter $\hat{b}(\mathbf{x})$ during training of **ResNet-18** on CIFAR-10, with batch size $b \in \{16, 64, 256, 1024\}$.

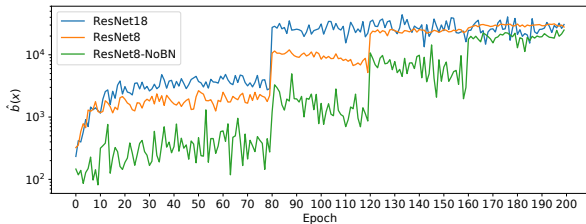


Figure 6: Evolution of the critical parameter $\hat{b}(\mathbf{x})$ during training **ResNet-8** and **ResNet-18** on CIFAR-10 with batch size $b = 256$.

lower throughout the training than with batch norm enabled. Note that while we use different batch sizes in training, we compute all the metrics such as $\xi(\mathbf{x})$ and $\nabla f(\mathbf{x})$ with batch size 256.

Next, we use a similar setup as in (Shallue et al., 2019) and measure the evolution of $\hat{b}(\mathbf{x})$ when using learning rate decay to train ResNet-18 and ResNet-8 with and without batch norm, depicted in Figure 6. We use 0.1 initial step size and decay by a factor of 0.1 at epochs 80, 120, and 160. The estimated value of $\hat{b}(\mathbf{x})$ increases after each learning rate decay. A decay in learning rate results in a sudden decrease in the gradient’s norm, lowering the target error for which $\hat{b}(\mathbf{x})$ estimates the critical batch size. The change in $\hat{b}(\mathbf{x})$ may therefore be justified by the sudden decrease in the target error.

7.3 Large Batch Speedup Analysis

In the previous subsection we studied the evolution of the estimator $\hat{b}(\mathbf{x})$ over training. Since $\hat{b}(\mathbf{x})$ provides a lower bound for b_{crit} , We obtain a estimator of the critical batch size by taking the maximal observed value until reaching a certain target accuracy, $\hat{b}_{\text{crit}} = \max_i \hat{b}(\mathbf{x}_i)$. We now investigate, how this estimate correlates with the speedup saturation observed in practice.

We train ResNet-8 without Batch Normalization with different batch sizes and separately tuned the step size

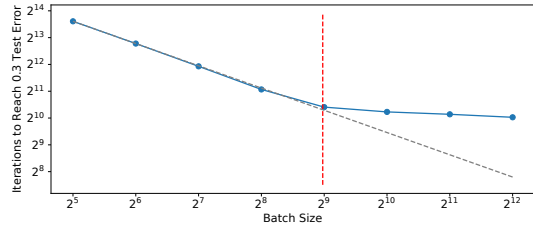


Figure 7: **Linear speedup up to batch size \hat{b}_{crit}** . The number of iterations to reach 0.3 test error with **ResNet-8** on CIFAR-10 without batch normalization for batch size $b \in \{2^5, \dots, 2^{12}\}$. The red line shows the estimated \hat{b}_{crit} .

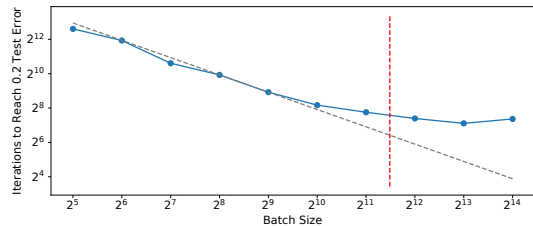


Figure 8: The number of iterations to reach 0.2 test error with **ResNet-18** on CIFAR-10 without batch normalization for batch size $b \in \{2^5, \dots, 2^{14}\}$. The red line shows the estimated \hat{b}_{crit} .

for each batch size. For each batch size, we trained the network until reaching 70% test accuracy (as in Shallue et al., 2019). We plot the number of steps (iterations) for each batch size overlaid with the value we estimated for \hat{b}_{crit} in Figure 7. Our result matches with the previous findings of (Shallue et al., 2019). We repeat the same procedure for ResNet-18 with Batch Normalization and train until reaching 80% test accuracy. To save computational costs, we only use a subset of batch sizes for estimation of $\hat{b}(\mathbf{x})$. The results are depicted in Figure 8.

8 Conclusion

We introduced a universal parameter that measures the critical level of parallelism (such as e.g. batch size, or delays) of stochastic optimization problems that allows for near-linear parallel speedup efficiency. Our notion extends and refines prior notions that could not explain speedup saturation beyond a *constant* critical batch size, closely matching empirical observations. Our measurements on deep learning tasks confirm that our proposed metric provides a meaningful estimate also on deep learning tasks. As future directions we leave it to extend the theory to refined notions of *locally* critical batch sizes (as e.g. considered in Section 7.2, or in Yin et al. 2018; Jain et al. 2018) and to study theoretically the generalization gap in large batch training (Keskar et al., 2017).

References

- Alekh Agarwal and John C Duchi. Distributed delayed stochastic optimization. In *NIPS - Advances in Neural Information Processing Systems 24*, pages 873–881. Curran Associates, Inc., 2011.
- Dan Alistarh, Demjan Grubic, Jerry Li, Ryota Tomioka, and Milan Vojnovic. QSGD: Communication-efficient SGD via gradient quantization and encoding. In *NIPS - Advances in Neural Information Processing Systems 30*, pages 1709–1720. Curran Associates, Inc., 2017.
- Dan Alistarh, Torsten Hoefer, Mikael Johansson, Nikola Konstantinov, Sarit Khirirat, and Cedric Renggli. The convergence of sparsified gradient methods. In *NeurIPS - Advances in Neural Information Processing Systems 31*, pages 5977–5987. Curran Associates, Inc., 2018.
- Yossi Arjevani, Ohad Shamir, and Nathan Srebro. A tight convergence analysis for stochastic gradient descent with delayed updates. In *ALT - 31st International Conference on Algorithmic Learning Theory*, volume 117, pages 111–132. PMLR, 2020.
- Dimitri P. Bertsekas and John N. Tsitsiklis. *Parallel and Distributed Computation: Numerical Methods*. Prentice-Hall, Inc., USA, 1989. ISBN 0136487009.
- L. Bottou, F. Curtis, and J. Nocedal. Optimization methods for large-scale machine learning. *SIAM Review*, 60(2):223–311, 2018. doi: 10.1137/16M1080173.
- Léon Bottou. Large-scale machine learning with stochastic gradient descent. In Yves Lechevallier and Gilbert Saporta, editors, *Proceedings of COMPSTAT’2010*, pages 177–186, Heidelberg, 2010. Physica-Verlag HD. ISBN 978-3-7908-2604-3.
- Rosa Candela, Giulio Franzese, Maurizio Filippone, and Pietro Michiardi. Sparsification as a remedy for staleness in distributed asynchronous SGD. *arXiv preprint arXiv:1910.09466*, 2019.
- V. Cevher and B. Công Vũ. On the linear convergence of the stochastic gradient method with constant step-size. *Optimization Letters*, 13(5):1177–1187, 2019.
- Sorathan Chaturapruek, John C Duchi, and Christopher Ré. Asynchronous stochastic convex optimization: the noise is in the noise and SGD don’t care. In *NIPS - Advances in Neural Information Processing Systems 28*, pages 1531–1539. Curran Associates, Inc., 2015.
- Lingjiao Chen, Hongyi Wang, Jinman Zhao, Dimitris Papailiopoulos, and Paraschos Koutris. The effect of network width on the performance of large-batch training. In *Advances in Neural Information Processing Systems 31*, pages 9302–9309. Curran Associates, Inc., 2018.
- Christopher M De Sa, Ce Zhang, Kunle Olukotun, Christopher Ré, and Christopher Ré. Taming the wild: A unified analysis of hogwild-style algorithms. In *NIPS - Advances in Neural Information Processing Systems 28*, pages 2674–2682. Curran Associates, Inc., 2015.
- Jeffrey Dean, Greg Corrado, Rajat Monga, Kai Chen, Matthieu Devin, Mark Mao, Marc D’aurelio Ranzato, Andrew Senior, Paul Tucker, Ke Yang, Quoc V. Le, and Andrew Y. Ng. Large scale distributed deep networks. In *NIPS - Advances in Neural Information Processing Systems 25*, pages 1223–1231. Curran Associates, Inc., 2012.
- Ofer Dekel, Ran Gilad-Bachrach, Ohad Shamir, and Lin Xiao. Optimal distributed online prediction using mini-batches. *Journal of Machine Learning Research (JMLR)*, 13(1):165–202, January 2012. ISSN 1532-4435.
- John Duchi, Michael I Jordan, and Brendan McMahan. Estimation, optimization, and parallelism when data is sparse. In *NIPS - Advances in Neural Information Processing Systems 26*, pages 2832–2840. Curran Associates, Inc., 2013.
- Rayan Elalamy, Sebastian U. Stich, and Martin Jaggi. Convergence analysis for Hogwild! under less restrictive assumptions. *EPFL Semester Project*, 2020.
- Michael P. Friedlander and Mark Schmidt. Hybrid deterministic-stochastic methods for data fitting. *SIAM Journal on Scientific Computing*, 34(3):A1380–A1405, 2012. doi: 10.1137/110830629.
- Priya Goyal, Piotr Dollár, Ross B. Girshick, Pieter Noordhuis, Lukasz Wesolowski, Aapo Kyrola, Andrew Tulloch, Yangqing Jia, and Kaiming He. Accurate, large mini-batch SGD: training ImageNet in 1 hour. *arXiv preprint arXiv:1706.02677*, 2017.
- Robert Hannah and Wotao Yin. On unbounded delays in asynchronous parallel fixed-point algorithms. *Journal of Scientific Computing*, 76(1):299–326, Jul 2018. doi: 10.1007/s10915-017-0628-z.
- Kaiming He, Xiangyu Zhang, Shaoqing Ren, and Jian Sun. Deep residual learning for image recognition. In *Proceedings of the IEEE Conference on Computer Vision and Pattern Recognition*, pages 770–778, 2016.
- Prateek Jain, Sham M. Kakade, Rahul Kidambi, Praneeth Netrapalli, and Aaron Sidford. Parallelizing stochastic gradient descent for least squares regression: Minibatching, averaging, and model misspecification. *Journal of Machine Learning Research (JMLR)*, 18(223):1–42, 2018.
- Peter Kairouz, H. Brendan McMahan, Brendan Avent, Aurélien Bellet, Mehdi Bennis, Arjun Nitin Bhagoji, Keith Bonawitz, Zachary Charles, Graham Cormode, Rachel Cummings, Rafael G. L. D’Oliveira, Salim El Rouayheb, David Evans, Josh Gardner, Zachary Garrett, Adrià Gascón, Badih Ghazi, Phillip B. Gibbons, Marco Gruteser, Zaid Harchaoui, Chaoyang He, Lie He, Zhouyuan Huo, Ben Hutchinson, Justin Hsu, Martin Jaggi, Tara Javidi, Gauri Joshi, Mikhail Khodak, Jakub Konečný, Aleksandra Korolova, Farinaz Koushanfar, Sanmi Koyejo, Tancrède Lepoint, Yang Liu, Prateek Mittal, Mehryar Mohri, Richard Nock, Ayfer Özgür, Rasmus Pagh, Mariana Raykova, Hang Qi, Daniel Ramage, Ramesh Raskar, Dawn Song, Weikang Song, Sebastian U. Stich, Ziteng Sun, Ananda Theertha Suresh, Florian Tramèr, Praneeth Vepakomma, Jianyu Wang, Li Xiong, Zheng Xu, Qiang Yang, Felix X. Yu, Han Yu, and Sen Zhao. Advances and open problems in federated learning. *arXiv preprint arXiv:1912.04977*, 2019.
- Nitish Shirish Keskar, Dheevatsa Mudigere, Jorge Nocedal, Mikhail Smelyanskiy, and Ping Tak Peter Tang. On large-batch training for deep learning: Generalization gap and sharp minima. *ICLR - International Conference on Learning Representations*, 2017.
- Alex Krizhevsky and Geoffrey Hinton. Learning multiple layers of features from tiny images. 2009.

- John Langford, Alex J. Smola, and Martin Zinkevich. Slow learners are fast. In *NIPS - Advances in Neural Information Processing Systems 22*, pages 2331–2339. Curran Associates, Inc., 2009.
- Remi Leblond, Fabian Pedregosa, and Simon Lacoste-Julien. Improved asynchronous parallel optimization analysis for stochastic incremental methods. *Journal of Machine Learning Research (JMLR)*, 19(81):1–68, 2018.
- Namhoon Lee, Philip HS Torr, and Martin Jaggi. Data parallelism in training sparse neural networks. *arXiv preprint arXiv:2003.11316*, 2020.
- Si Yuan Ma, Raef Bassily, and Mikhail Belkin. The power of interpolation: Understanding the effectiveness of SGD in modern over-parametrized learning. In *ICML - Proceedings of the 35th International Conference on Machine Learning*, volume 80, pages 3325–3334. PMLR, 2018.
- Horia Mania, Xinghao Pan, Dimitris Papailiopoulos, Benjamin Recht, Kannan Ramchandran, and Michael I. Jordan. Perturbed iterate analysis for asynchronous stochastic optimization. *SIAM Journal on Optimization*, 27(4):2202–2229, 2017.
- Brendan McMahan, Eider Moore, Daniel Ramage, Seth Hampson, and Blaise Agueria y Arcas. Communication-efficient learning of deep networks from decentralized data. In *AISTATS - 20th International Conference on Artificial Intelligence and Statistics*, volume 54, pages 1273–1282. PMLR, 2017.
- A. S. Nemirovski and D. B. Yudin. *Problem Complexity and Method Efficiency in Optimization*. John Wiley & Sons, Inc., New York, NY, USA, 1983.
- Yurii Nesterov. *Introductory Lectures on Convex Optimization*, volume 87 of *Springer Science & Business Media*. Springer US, Boston, MA, 2004.
- Lam M. Nguyen, Phuong Ha Nguyen, Peter Richtárik, Katya Scheinberg, Martin Takáč, and Marten van Dijk. New convergence aspects of stochastic gradient algorithms. *Journal of Machine Learning Research (JMLR)*, 2019.
- Feng Niu, Benjamin Recht, Christopher Re, and Stephen Wright. Hogwild: A lock-free approach to parallelizing stochastic gradient descent. In *NIPS - Advances in Neural Information Processing Systems 24*, pages 693–701. Curran Associates, Inc., 2011. references referring to arxiv/1106.5730v2 version.
- Herbert Robbins and Sutton Monro. A Stochastic Approximation Method. *The Annals of Mathematical Statistics*, 22(3):400–407, September 1951.
- Karthik A. Sankararaman, Soham De, Zheng Xu, W. Ronny Huang, and Tom Goldstein. The impact of neural network overparameterization on gradient confusion and stochastic gradient descent. *arXiv preprint arXiv:1904.06963*, 2019.
- Christopher J. Shallue, Jaehoon Lee, Joseph Antognini, Jascha Sohl-Dickstein, Roy Frostig, and George E. Dahl. Measuring the effects of data parallelism on neural network training. *Journal of Machine Learning Research*, 20(112):1–49, 2019.
- Suvrit Sra, Adams Wei Yu, Mu Li, and Alex Smola. Adadelay: Delay adaptive distributed stochastic optimization. In *AISTATS - 19th International Conference on Artificial Intelligence and Statistics*, volume 51, pages 957–965. PMLR, 09–11 May 2016.
- Sebastian U. Stich and Sai P. Karimireddy. The error-feedback framework: Better rates for SGD with delayed gradients and compressed communication. *Journal of Machine Learning Research (JMLR)*, 2020.
- J. Tsitsiklis, D. Bertsekas, and M. Athans. Distributed asynchronous deterministic and stochastic gradient optimization algorithms. *IEEE Transactions on Automatic Control*, 31(9):803–812, Sep. 1986. ISSN 2334-3303. doi: 10.1109/TAC.1986.1104412.
- Dong Yin, Ashwin Pananjady, Max Lam, Dimitris Papailiopoulos, Kannan Ramchandran, and Peter Bartlett. Gradient diversity: a key ingredient for scalable distributed learning. In Amos Storkey and Fernando Perez-Cruz, editors, *AISTATS - 21st International Conference on Artificial Intelligence and Statistics*, volume 84 of *PMLR*, pages 1998–2007. PMLR, 09–11 Apr 2018.
- Martin Zinkevich, Markus Weimer, Lihong Li, and Alex J Smola. Parallelized stochastic gradient descent. In *NeurIPS - Advances in neural information processing systems*, pages 2595–2603, 2010.

A On the proof of Theorem 1

For the proof of Theorem 1 we resort to techniques and results that have been developed in prior works and that can easily be adapted to the setting considered here, in particular (Stich and Karimireddy, 2020, Theorem 15). This theorem addresses the particular case when the gradients in Algorithm 1 are all delayed by a delay of *exactly* τ (a.k.a. *delayed SGD*). In contrast, we consider here the setting where coordinates of the gradients can be delayed independently, delays do not follow a particular order and reading of the variable \mathbf{x} from the memory can be inconsistent. However, the proof in (Stich and Karimireddy, 2020) can easily be adapted to our more general setting (as also observed in Elalamy et al., 2020) and we do not claim much novelty here—except of explicitly stating this generalization.

A.1 Proof Overview

The proof in (Stich and Karimireddy, 2020) for the convex case follows by refining the perturbed iterated framework, developed in (Mania et al., 2017) and extended in (Leblond et al., 2018). A key ingredient in the proof is to consider a (virtual, ghost) sequence

$$\tilde{\mathbf{x}}_{t+1} := \tilde{\mathbf{x}}_t - \gamma_t \mathbf{g}_t$$

with $\mathbf{g}_t = \mathbf{g}_t(\mathbf{x}_t)$. In the following we resort—for the ease of presentation—to constant step sizes $\gamma_t \equiv \gamma$.

For instance for convex functions, it can be shown (Stich and Karimireddy, 2020, Lemma 7) that the perturbed iterates satisfy

$$\mathbb{E}\|\tilde{\mathbf{x}}_{t+1} - \mathbf{x}^*\|^2 \leq \left(1 - \frac{\mu\gamma}{2}\right) \mathbb{E}\|\tilde{\mathbf{x}}_t - \mathbf{x}^*\|^2 - \frac{\gamma}{2} (\mathbb{E}f(\mathbf{x}_t) - f^*) + \gamma^2 \sigma^2 + 3L\gamma \underbrace{\mathbb{E}\|\mathbf{x}_t - \tilde{\mathbf{x}}_t\|^2}_{=: R_t}, \quad (10)$$

and for non-convex functions (Stich and Karimireddy, 2020, Lemma 8):

$$\mathbb{E}f(\tilde{\mathbf{x}}_{t+1}) \leq \mathbb{E}f(\mathbf{x}_t) - \frac{\gamma}{4} \mathbb{E}\|\nabla f(\mathbf{x}_t)\|^2 + \frac{\gamma^2 L}{2} \sigma^2 + \frac{\gamma L}{2} \underbrace{\mathbb{E}\|\mathbf{x}_t - \tilde{\mathbf{x}}_t\|^2}_{=: R_t}. \quad (11)$$

A.2 Bound on R_t in (Stich and Karimireddy, 2020)

Stich and Karimireddy (2020) analyze the convergence of a *delayed gradient method*, as introduced in (Arjevani et al., 2020) and provide an upper bound for the value of R_t .

Lemma 3 (Stich and Karimireddy 2020, Lemma 10). *Let $\gamma \leq \frac{1}{10L(\tau+M)}$ and \mathbf{x}_t defined as $\mathbf{x}_{t+1} := \mathbf{x}_t - \gamma \mathbf{g}_{t-\tau}$ for $t \geq \tau$, and $\mathbf{x}_t = \mathbf{x}_0$ for $t \in \{0, \dots, \tau - 1\}$ (delayed SGD). Then*

$$R_t := \mathbb{E}[\|\mathbf{x}_t - \tilde{\mathbf{x}}_t\|^2] \leq \frac{1}{30L^2\tau} \sum_{k=(t-\tau)_+}^{t-1} \mathbb{E}\|\nabla f(\mathbf{x}_k)\|^2 + \frac{2}{3L} \gamma \sigma^2 =: \Theta_{\text{SK}}. \quad (12)$$

A.3 Bound on R_t under τ bounded parallelism

We now switch to our setting and derive a similar bound on R_t that holds for the more general class of algorithms considered in Theorem 1.

Lemma 4. *It holds*

$$R_t = \mathbb{E}\|\mathbf{x}_t - \tilde{\mathbf{x}}_t\|^2 \leq 2\gamma^2(\tau + M) \sum_{k=(t-\tau)_+}^{t-1} \mathbb{E}\|\nabla f(\mathbf{x}_k)\|^2 + 2\gamma^2\tau\sigma^2.$$

and in particular for $\gamma \leq \gamma_{\text{crit}} = \frac{1}{10L(M+\tau)}$

$$R_t \leq \frac{1}{50L^2\tau} \sum_{k=(t-\tau)_+}^{t-1} \mathbb{E}\|\nabla f(\mathbf{x}_k)\|^2 + \frac{1}{5L} \gamma \sigma^2 =: \Theta_{\text{SMJ}}. \quad (13)$$

We observe that our bound provided in (13) is smaller than the bound provided in (12), i.e., $\Theta_{\text{SMJ}} \leq \Theta_{\text{SK}}$. Therefore, the proof of Theorem 1 now follows from (Stich and Karimireddy, 2020, Theorem 16) (that only relies on the weaker bound Θ_{SK}).

Proof of Lemma 4. First, we observe that by definition of \mathbf{x}_t and $\tilde{\mathbf{x}}_t$ and the maximal overlap τ , we can write

$$\|\mathbf{x}_t - \tilde{\mathbf{x}}_t\|^2 := \|\gamma \sum_{k < t} (\mathbf{J}_k^t - \mathbf{I}_d) \mathbf{g}_k\|^2 = \|\gamma \sum_{k=(t-\tau)_+}^{t-1} (\mathbf{J}_k^t - \mathbf{I}_d) \mathbf{g}_k\|^2, \quad (14)$$

where $\mathbf{g}_k := \nabla f(\mathbf{x}_k) + \boldsymbol{\xi}_k$ for zero-mean noise terms. Therefore

$$\begin{aligned} \mathbb{E}\|\mathbf{x}_t - \tilde{\mathbf{x}}_t\|^2 &\stackrel{\textcircled{1}}{\leq} 2\gamma^2 \left(\mathbb{E}\left\| \sum_{k=(t-\tau)_+}^{t-1} (\mathbf{J}_k^t - \mathbf{I}_d) \nabla f(\mathbf{x}_k) \right\|^2 + \mathbb{E}\left\| \sum_{k=(t-\tau)_+}^{t-1} (\mathbf{J}_k^t - \mathbf{I}_d) \boldsymbol{\xi}_k \right\|^2 \right) \\ &\stackrel{\textcircled{2}}{\leq} 2\gamma^2 \left(\tau \sum_{k=(t-\tau)_+}^{t-1} \mathbb{E}\|(\mathbf{J}_k^t - \mathbf{I}_d) \nabla f(\mathbf{x}_k)\|^2 + \sum_{k=(t-\tau)_+}^{t-1} \mathbb{E}\|(\mathbf{J}_k^t - \mathbf{I}_d) \boldsymbol{\xi}_k\|^2 \right) \\ &\stackrel{\textcircled{3}}{\leq} 2\gamma^2 \left(\tau \sum_{k=(t-\tau)_+}^{t-1} \mathbb{E}\|\nabla f(\mathbf{x}_k)\|^2 + \sum_{k=(t-\tau)_+}^{t-1} \mathbb{E}\|\boldsymbol{\xi}_k\|^2 \right) \\ &\stackrel{\textcircled{4}}{\leq} 2\gamma^2 \left((\tau + M) \sum_{k=(t-\tau)_+}^{t-1} \mathbb{E}\|\nabla f(\mathbf{x}_k)\|^2 + \tau\sigma^2 \right), \end{aligned}$$

where we used $\textcircled{1}$ $\|\mathbf{a} + \mathbf{b}\|^2 \leq 2\|\mathbf{a}\|^2 + 2\|\mathbf{b}\|^2$, $\textcircled{2}$ $\|\sum_{i=1}^{\tau} \mathbf{a}_i\|^2 \leq \tau \sum_{i=1}^{\tau} \|\mathbf{a}_i\|^2$, and $\mathbb{E}\|\sum_{i=1}^{\tau} \boldsymbol{\xi}_i\|^2 = \sum_{i=1}^{\tau} \mathbb{E}\|\boldsymbol{\xi}_i\|^2$, $\textcircled{3}$ $\|(\mathbf{J}_k^t - \mathbf{I}_d) \nabla f(\mathbf{x}_k)\|^2 \leq \|\mathbf{J}_k^t - \mathbf{I}_d\|^2 \|\nabla f(\mathbf{x}_k)\|^2 \leq M \|\nabla f(\mathbf{x}_k)\|^2$, $\textcircled{4}$ $\mathbb{E}\|\boldsymbol{\xi}_k\|^2 \leq M \|\nabla f(\mathbf{x}_k)\|^2 + \sigma^2$. \square

A.4 Concluding the proof

As mentioned above, the proof now follows directly from (Stich and Karimireddy, 2020, Theorem 16). To make this paper more self-contained, we illustrate the remaining steps for the case of non-convex functions.

For the non-convex case, equation (11) gives us the progress of one step. Using notation $r_t := 4\mathbb{E}(f(\tilde{\mathbf{x}}_t) - f^*)$, $s_t := \mathbb{E}\|\nabla f(\mathbf{x}_t)\|^2$, and $c = 4L\sigma^2$ we have

$$\begin{aligned} \frac{1}{4T} \sum_{t=0}^T s_t &\stackrel{\textcircled{11}}{\leq} \frac{1}{T} \sum_{t=0}^T \left(\frac{r_t}{4\gamma_t} - \frac{r_{t+1}}{4\gamma} + \frac{\gamma c}{8} \right) + \frac{L^2}{2T} \sum_{t=0}^T \mathbb{E}\|\mathbf{x}_t - \tilde{\mathbf{x}}_t\|^2 \\ &\stackrel{(\Theta_{\text{SMJ}} \leq \Theta_{\text{SK}})}{\stackrel{\textcircled{12}}{\leq}} \frac{1}{T} \sum_{t=0}^T \left(\frac{r_t}{4\gamma} - \frac{r_{t+1}}{4\gamma} + \frac{\gamma c}{8} \right) + \frac{L^2}{2T} \sum_{t=0}^T \left(\frac{1}{15L^2} s_t + \frac{\gamma c}{4L^2} \right). \end{aligned}$$

The above equation can be simplified as:

$$\frac{1}{5T} \sum_{t=0}^T s_t \leq \frac{1}{T} \sum_{t=0}^T \left(\frac{r_t}{4\gamma} - \frac{r_{t+1}}{4\gamma} + \frac{\gamma c}{4} \right) \leq \frac{r_0}{4\gamma T} + \frac{\gamma c}{4}.$$

Now, the claimed bound follows by choosing the optimal stepsize $\gamma \leq \gamma_{\text{crit}}$ that minimizes the right hand side. For this refer e.g. to (Stich and Karimireddy, 2020, Lemma 14) or (Arjevani et al., 2020).

The proof for the convex cases start from the one step progress provided in (10) instead, and proceed similarly.

B Additional numerical experiments

In this section we report additional empirical results for the setting considered in Section 7.1. We consider three algorithms with the same level of parallelism: mini-batch SGD as considered in the main text, and two implementations of SGD with delayed updates.

B.1 On the estimator $\hat{b}(\mathbf{x})$

Note that

$$1 + \frac{\sigma_*^2}{\max\{\hat{\epsilon}_T, \|\nabla f(\mathbf{x})\|^2\}} + M \geq 1 + \frac{M\|\nabla f(\mathbf{x})\|^2 + \sigma_*^2}{\|\nabla f(\mathbf{x})\|^2 + \hat{\epsilon}_T} \stackrel{(5)}{\geq} \hat{b}(\mathbf{x}). \quad (15)$$

Moreover, for $\tilde{\epsilon} := \max\{\hat{\epsilon}_T, \|\nabla f(\mathbf{x})\|^2\}$,

$$1 + \frac{\sigma_*^2}{\tilde{\epsilon}} + M \leq 1 + \sup_{\|\nabla f(\mathbf{x})\|^2 \leq \tilde{\epsilon}} \frac{\mathbb{E}\|\boldsymbol{\xi}(\mathbf{x})\|^2}{\tilde{\epsilon}} + \sup_{\|\nabla f(\mathbf{x})\|^2 \geq \tilde{\epsilon}} \frac{\mathbb{E}\|\boldsymbol{\xi}(\mathbf{x})\|^2}{\|\nabla f(\mathbf{x})\|^2} \quad (16)$$

$$\leq 1 + 2 \sup_{\mathbf{x} \in \mathbb{R}^d} \frac{\mathbb{E}\|\boldsymbol{\xi}(\mathbf{x})\|^2}{\tilde{\epsilon} + \|\nabla f(\mathbf{x})\|^2} + 2 \sup_{\mathbf{x} \in \mathbb{R}^d} \frac{\mathbb{E}\|\boldsymbol{\xi}(\mathbf{x})\|^2}{\tilde{\epsilon} + \|\nabla f(\mathbf{x})\|^2} \quad (17)$$

$$\leq 4 \sup_{\mathbf{x} \in \mathbb{R}^d} \hat{b}(\mathbf{x}). \quad (18)$$

This method of measuring the critical batch size might not be too accurate. We use this estimator only to show that our theoretical findings match our observations in practice and to show how they can be used to explain phenomena such as critical batch size and scaling of learning rate. We leave finding a more accurate and online method for measuring the critical batch size as a possible future work.

B.2 Mini-batch SGD

We consider standard mini-batch SGD, for batch size $b \geq 1$,

$$\mathbf{x}_{t+b} = \mathbf{x}_t - \frac{\gamma_{\text{bm}}}{b} \sum_{i=1}^b \mathbf{g}^i(\mathbf{x}_t),$$

where $\mathbf{g}^i(\mathbf{x}_t)$ for $i \in [b]$ denotes independently sampled stochastic gradients.

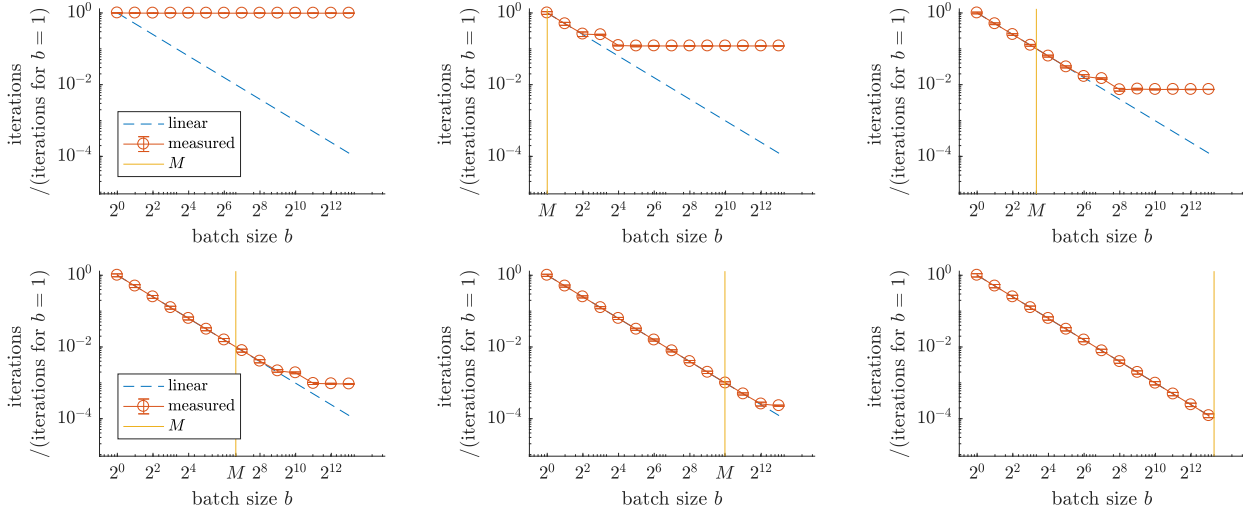


Figure 9: **Scaling (Mini-batch SGD)**. Parallel speedup for various batch sizes $b \in \{2^0, \dots, 2^{14}\}$ and problem instances with $M \in \{0, 1, 10\}$ (top) and $M \in \{100, 1000, 10000\}$ (bottom), on the synthetic optimization problem described in Section 7.1, averaged over three random seeds (depicting mean and \pm SD). Plots depict number of iterations (i.e. parallel running time $\frac{1}{b}T(b, \epsilon)$), normalized by $T(1, \epsilon)$, required to reach the target accuracy with tuned optimal learning rates.

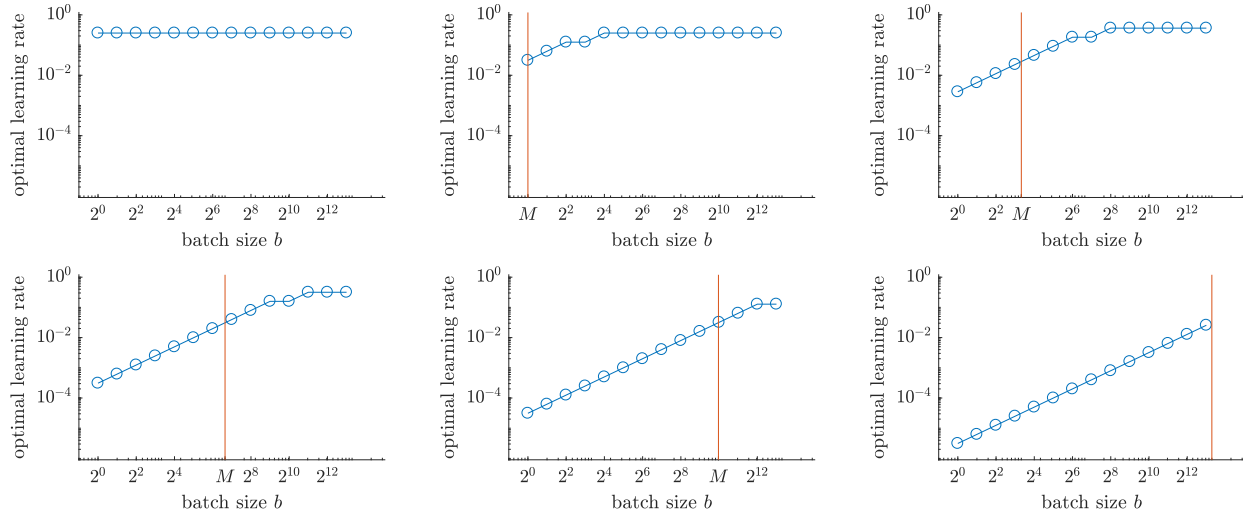


Figure 10: **Optimal learning rate γ_{mb} for mini-batch SGD** for the results reported in Figure 9.

B.3 Delayed SGD (coordinate-wise random delays)

In this section we consider SGD with delayed updates. Concretely, we simulate the case where each coordinate $[\mathbf{g}(\mathbf{x}_t)]_v$, $v \in [d]$ is delayed for a delay $\tau_{t,v} \sim_{\text{u.a.r.}} [\tau]$. This can be seen as a simplistic modeling of Hogwild! (Niu et al., 2011), though in practical settings the delays might be correlated. The update can be written as

$$\mathbf{x}_{t+1} = \mathbf{x}_t - \frac{\gamma_{\text{HW}}}{\tau} \sum_{i=t+1-\tau}^t \mathbf{P}_i^t \mathbf{g}_i$$

where $\mathbf{g}_t := \mathbf{g}(\mathbf{x}_t)$ stochastic gradients (sampled at iteration t), and \mathbf{P}_i^t are diagonal matrices with $\sum_{k \geq t} \mathbf{P}_i^k = \mathbf{I}_d$, $(\mathbf{P}_i^t)_{vv} = 1$ if $[\mathbf{g}_t]_v$ is written at iteration $i \geq t$ and $(\mathbf{P}_i^t)_{vv} = 0$ otherwise.

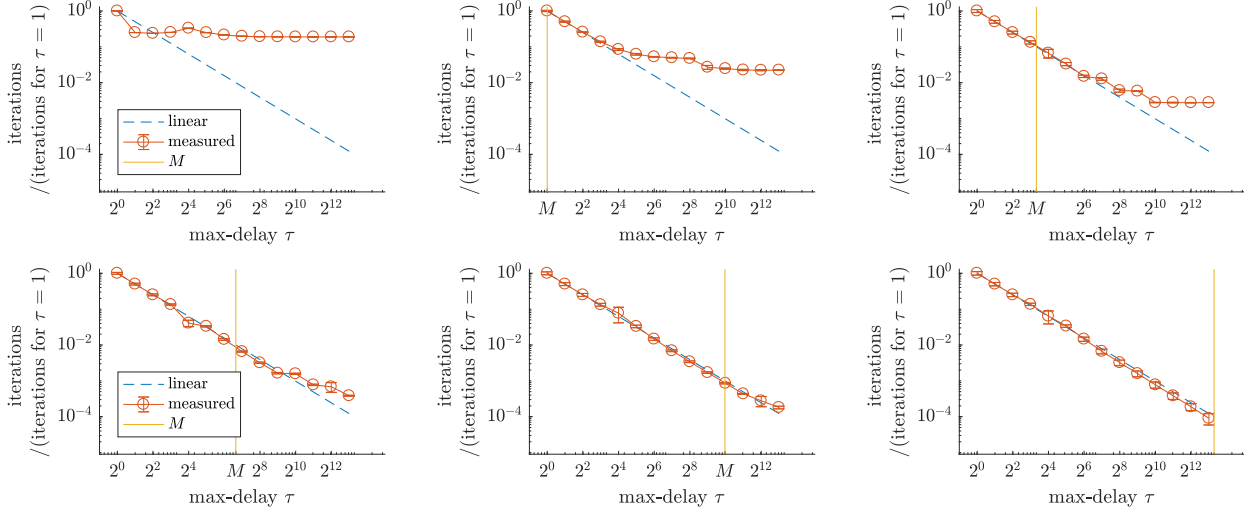


Figure 11: **Scaling of SGD with coordinate-wise delayed updates (Hogwild!).** Parallel speedup for various batch sizes/delay values $b \in \{2^0, \dots, 2^{14}\}$ and problem instances with $M \in \{0, 1, 10\}$ (top) and $M \in \{100, 1000, 10000\}$ (bottom), on the synthetic optimization problem described in Section 7.1, averaged over three random seeds (depicting mean and \pm SD). Plots depict number of iterations (i.e. parallel running time $\frac{1}{b}T(b, \epsilon)$), normalized by $T(1, \epsilon)$, required to reach the target accuracy with tuned optimal learning rates.

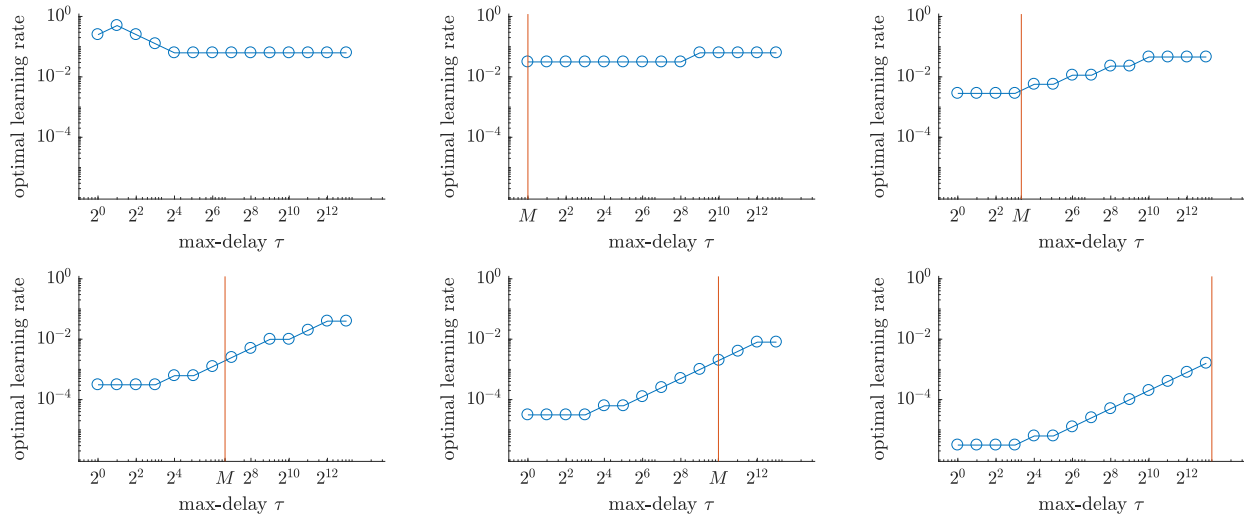


Figure 12: **Optimal learning rate γ_{HW} for Hogwild!** for the results reported in Figure 11.

B.4 Delayed SGD (worst case delays)

In this section we consider SGD with delayed updates (Arjevani et al., 2020). Concretely, we assume each gradient update is delayed by exactly τ iterations. For $t \geq \tau$, the update can be written as

$$\mathbf{x}_{t+1} = \mathbf{x}_t - \frac{\gamma_d}{\tau} \mathbf{g}(\mathbf{x}_{t+1-\tau}),$$

with $\mathbf{x}_i = \mathbf{x}_0$ for $i \in [\tau - 1]$.

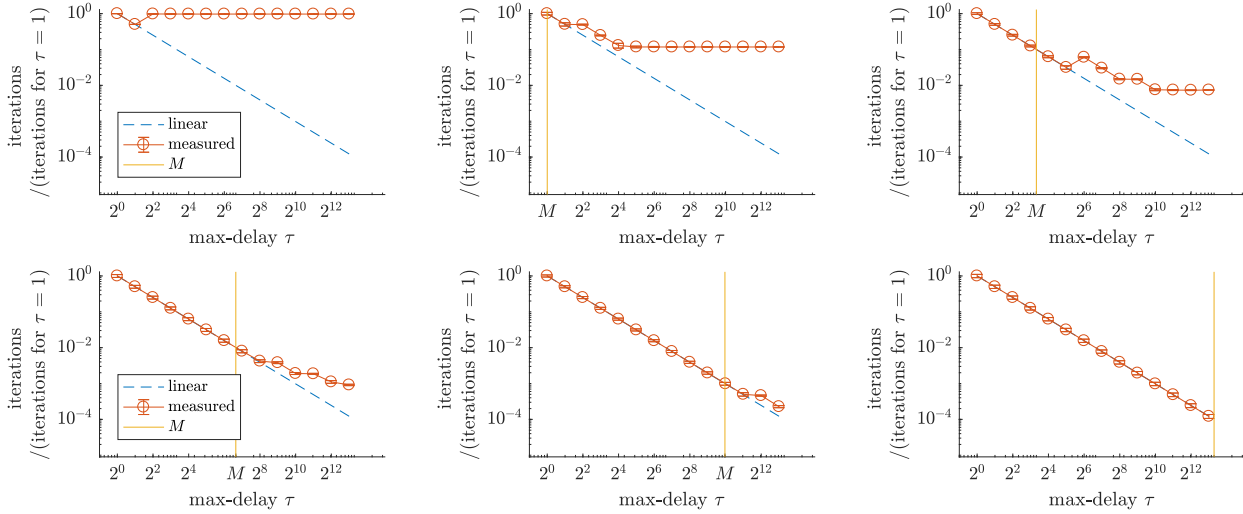


Figure 13: **Scaling of delayed SGD.** Parallel speedup for various delay values $\tau \in \{2^0, \dots, 2^{14}\}$ and problem instances with $M \in \{0, 1, 10\}$ (top) and $M \in \{100, 1000, 10000\}$ (bottom), on the synthetic optimization problem described in Section 7.1, averaged over three random seeds (depicting mean and \pm SD). Plots depict number of iterations (i.e. parallel running time $\frac{1}{b}T(b, \epsilon)$), normalized by $T(1, \epsilon)$, required to reach the target accuracy with tuned optimal learning rates.

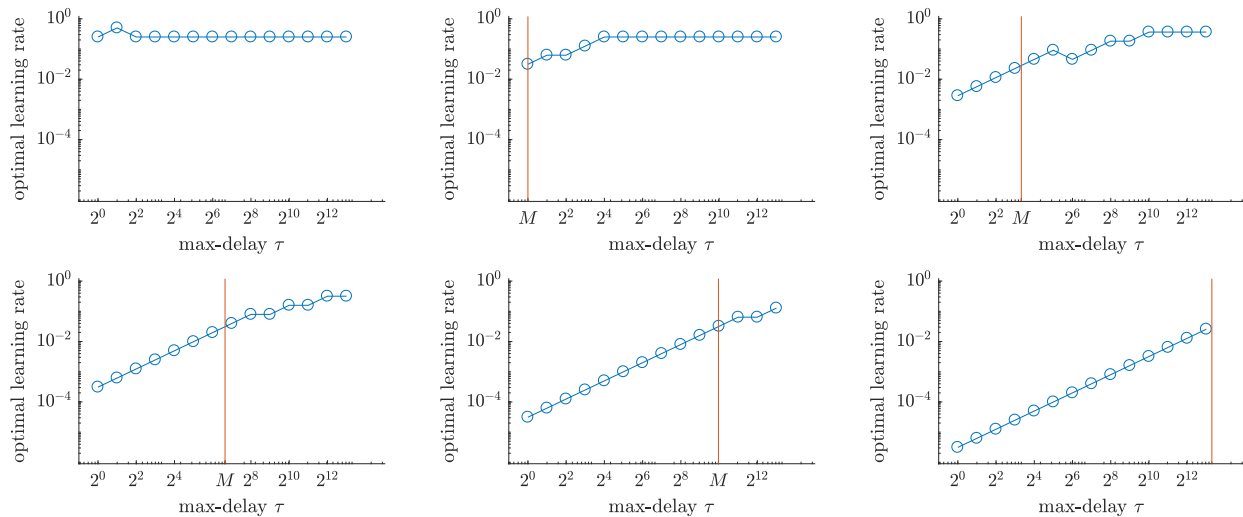


Figure 14: **Optimal learning rate γ_d for delayed SGD** for the results reported in Figure 13.

B.5 Hyperparameters for Deep Learning Experiments

For Figures 7 and 8, we tune the learning rate for each batch size. In particular, for ResNet-8, we use as step size, 0.4 when batch size is 32, 0.2 when batch size is 64 and 0.05 for all other batch sizes. The step size was chosen from the set $\{0.005, 0.05, 0.02, 0.1, 0.2, 0.4\}$.

Critical Parameters for Scalable Distributed Learning

For ResNet-18, we use as step size, 0.02 when batch size is 32, 0.04 when batch size is 64 and 0.1 for all other batch sizes. The step size was chosen from the set $\{0.005, 0.02, 0.05, 0.1\}$.